European Journal of Mechanics / A Solids 83 (2020) 104033

Contents lists available at ScienceDirect

European Journal of Mechanics / A Solids

journal homepage: http://www.elsevier.com/locate/ejmsol

Finite integral transform method for analytical solutions of static problems of cylindrical shell panels

Dongqi An [a], Dian Xu [a], Zhuofan Ni [a], Yewang Su [b,c,a], Bo Wang [a], Rui Li [a,*]

[a] State Key Laboratory of Structural Analysis for Industrial Equipment, Department of Engineering Mechanics, and International Research Center for Computational Mechanics, Dalian University of Technology, Dalian, 116024, China
[b] State Key Laboratory of Nonlinear Mechanics, Institute of Mechanics, Chinese Academy of Sciences, Beijing, 100190, China
[c] School of Engineering Science, University of Chinese Academy of Sciences, Beijing, 100049, China

ARTICLE INFO

Keywords:
Finite integral transform
Analytical solution
Cylindrical shell
Static problem

ABSTRACT

In this paper, a double finite integral transform method is developed for analytical bending solutions of non-Lévy-type cylindrical shell panels without a free edge that were not obtained by classical semi-inverse methods. Three double finite integral transforms are imposed on the governing high-order partial differential equations, which, with some boundary conditions, yields the relationship between the transformed quantities and specific unknowns. Incorporating the inversions into the remaining boundary conditions leads to systems of linear algebraic equations, which determine the final analytical solutions. Comprehensive benchmark results for representative cylindrical shell panels with combinations of clamped and simply supported edges are presented, which are well validated by satisfactory agreement with other solution methods. Due to its rigorous and straightforward solution procedure, the developed method provides a solid easy-to-implement approach for exploring new analytical solutions.

1. Introduction

Shells are important load-bearing components with broad applications to engineering structures such as buildings, aircrafts, pressure vessels and launch vehicles. Accordingly, the mechanical behaviors of shells have attracted extensive investigations for many years (Leissa, 1973; Timoshenko and Woinowsky-Krieger, 1959). Whichever theory is adopted, the mechanics problems of shells are reduced to solving the governing high-order partial differential equations (PDEs) subject to specific boundary conditions. Therefore, a critical issue is to develop feasible solution approaches, which generally fall into two categories, i.e., analytical and numerical. Compared with numerical solution methods, analytical ones were less developed due to the acknowledged mathematical difficulty in treating the complex boundary-value problems of the PDEs in a rigorous way. While various effective numerical methods have been proposed for shell problems, it is still necessary to explore analytical methods, which can not only provide benchmark theoretical solutions of permanent significance but can also explicitly capture the relationships between mechanical responses and inputs, thus are especially useful for rapid structural analysis, efficient parameter optimization and design.

Among lots of numerical methods available in the literature, the representative ones include the finite element method (FEM) (Achryya et al., 2009), finite strip method (Assaee and Hasani, 2015), boundary element method (Dirgantara and Aliabadi, 2012), differential cubature method (Mousavi and Aghdam, 2009), meshless method (Ferreira et al., 2011), strip layer method (Chen et al., 2013), etc. Compared with the numerical methods, there are much fewer analytical/semi-analytical methods reported for solving shell problems. Cinefra et al. (2010) derived the closed-form solutions of free vibration problems of simply supported multilayered shells made of functionally graded material. The proposed variable kinematic model was able to obtain exact values and to establish the accuracy of classical shell theories, especially for multilayered shells. H. Li et al. (2019) investigated the free vibration of uniform and stepped annular-spherical shells with general boundary conditions by using the Rayleigh-Ritz approach, where the displacement functions of shell segments consisted of the Jacobi polynomials along the axial direction and the standard Fourier series along the circumferential direction. The results showed that the method has good convergence and excellent accuracy. R. Li et al. (2019) proposed an analytical symplectic superposition method for analyzing the mechanical behaviors of plate and shell structures (Zheng et al., 2019). The

* Corresponding author.
E-mail address: ruili@dlut.edu.cn (R. Li).

https://doi.org/10.1016/j.euromechsol.2020.104033
Received 17 February 2020; Received in revised form 24 April 2020; Accepted 28 April 2020
Available online 11 May 2020

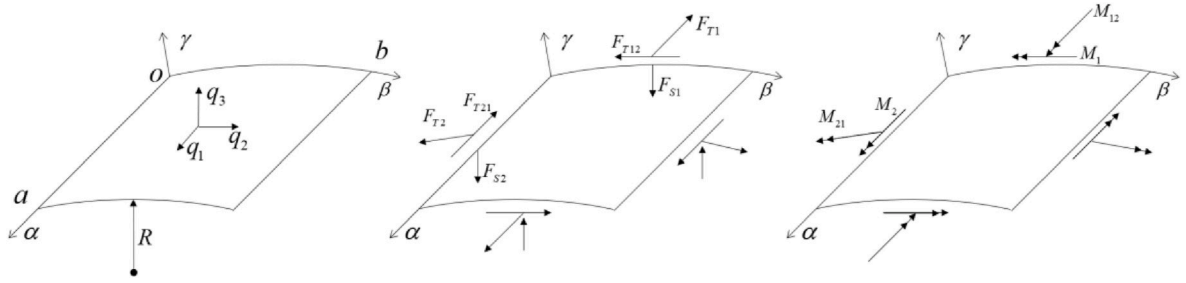

Fig. 1. A cylindrical shell panel in the $\alpha o\beta$ curvilinear coordinate system, with the directions of the positive external loads and internal forces indicated.

$$\left(\frac{\partial^2}{\partial\alpha^2}+\frac{1-\mu}{2}\frac{\partial^2}{\partial\beta^2}\right)u+\frac{1+\mu}{2}\frac{\partial^2 v}{\partial\alpha\partial\beta}+\frac{\mu}{R}\frac{\partial w}{\partial\alpha}=-\frac{1-\mu^2}{E\delta}q_1 \tag{1}$$

$$\frac{1+\mu}{2}\frac{\partial^2 u}{\partial\alpha\partial\beta}+\left(\frac{\partial^2}{\partial\beta^2}+\frac{1-\mu}{2}\frac{\partial^2}{\partial\alpha^2}\right)v+\frac{1}{R}\frac{\partial w}{\partial\beta}=-\frac{1-\mu^2}{E\delta}q_2 \tag{2}$$

$$\frac{\mu}{R}\frac{\partial u}{\partial\alpha}+\frac{1}{R}\frac{\partial v}{\partial\beta}+\frac{w}{R^2}+\frac{\delta^2}{12}\nabla^2\nabla^2 w=\frac{1-\mu^2}{E\delta}q_3 \tag{3}$$

method superposed several elaborated subproblems and was implemented within the Hamiltonian-system framework (Lim and Xu, 2010; Lim et al., 2009), showing rigorousness and high accuracy.

Integral transforms are a class of powerful methods that have found broad applications in solving the PDEs in various research fields such as heat transfer (Yang, 2016), convective diffusion (Cotta et al., 2013), nuclear physics (Ortakaya, 2012), fluid flow (Silva et al., 2011), signal process (Zhang et al., 2012), Tribology (Santos et al., 2012), and elasticity (Sneddon, 1975). Specifically, some recent progresses have been made on solving beam and plate problems by the finite integral transform method. An and Su (2011) employed the generalized finite integral transform technique to obtain a hybrid analytical-numerical solution for dynamic response of clamped axially moving beams. The approach can be either employed for benchmarking purposes or as an engineering simulation tool with exceptional computational performance. Matt (2013) combined classical and generalized finite integral transform methods for the transverse vibration analysis of a damaged simply supported beam. Numerical results obtained for a damaged beam demonstrated the accuracy, convergence and robustness of the combined strategy. Li et al. (2009) developed the finite integral transform method for exact bending solutions of fully clamped orthotropic rectangular thin plates, and extended it to buckling problems of thick plates (Ullah et al., 2019). Zhang et al. (2019) obtained new exact solutions for transverse vibration of rotationally-restrained orthotropic plates. Very recently, He et al. (2020a, 2020b) analyzed the free vibration of orthotropic rectangular thin plates with free edges and bending of the same plates with two opposite edges clamped by the generalized integral transform technique. Zhang et al. (2020) yielded the analytical free vibration solutions of orthotropic rectangular thin plates utilizing the similar technique. In spite of the advances in beam and plate analyses, there have been no reports, to the best of our knowledge, on extending such effective methods for analytical solutions of shell problems, which may be attributed to greater complexity of the shells.

In this study, we make the first attempt to further develop the finite integral transform method for analytical solutions of static problems of non-Lévy-type cylindrical shell panels without a free edge, i.e., those without two parallel edges simply supported, which cannot be obtained by a classical semi-inverse method. The current method is rigorous, straightforward, and with broad applicability, thus has great potential for accurate analysis of similar complex boundary-value problems of high-order PDEs. The rest of this paper is organized as follows. Section 2 presents the solution procedure based on three double finite integral transforms, which are imposed on the governing PDEs for bending of cylindrical shell panels. Inputting some boundary conditions, the relationship between the transforms of the displacements and specific unknowns is established. The inversions with those unknowns are substituted into the remaining boundary conditions to form infinite systems of linear simultaneous equations, the solutions of which finally yield the analytical solutions. Detailed derivations of fully clamped cylindrical shell panels serve as an example. Non-Lévy-type cylindrical shell panels with other combinations of clamped and simply supported edges are then solved in Section 3 to further demonstrate the generality of the developed method. In Section 4, comprehensive numerical results of cylindrical shell panels with different boundary conditions are tabulated in 11 tables, with 800 data listed for benchmark use, all of which are well validated by two available numerical and analytical methods. A convergence study is also implemented to consolidate the validity of the present solutions. Conclusions of the study are drawn in Section 5 as a closure.

2. Solution procedure based on finite integral transforms

Since this study focuses on cylindrical shell panels with combinations of clamped and simply supported edges, a convenient description of the boundary constraints is helpful. Using "C" and "S" as the abbreviations of "clamped" and "simply supported", a four-letter label is adopted to describe a panel according to the boundary constraints at the four edges, starting from the edge at $\beta = 0$ (Fig. 1) and proceeding counterclockwise.

2.1. Governing PDEs for bending of cylindrical shell panels

According to the well-accepted Donnell-Mushtari theory (Leissa, 1973), the governing PDEs for bending of a cylindrical shell panel as shown in Fig. 1 can be presented in the $\alpha o\beta$ curvilinear coordinate system as.where u, v, and w are the displacements along the α (longitudinal), β (circumferential), and γ (radial) directions, respectively, with q_1, q_2, and q_3 being the external load components in the corresponding directions; R is the radius of curvature along the β direction; E is the Young's modulus; μ is the Poisson's ratio; $\nabla^2 = \partial^2/\partial\alpha^2 + \partial^2/\partial\beta^2$ is the Laplacian operator. The dimensions of the panel in the α, β, and γ directions are denoted by a, b, and δ, respectively.

The displacements and internal forces are related by the following expressions:

Table 1
Convergence for the displacement solutions of CCCC cylindrical shell panels.

Displacement	Location	Number of series terms					SSM	FEM
		100	200	300	400	500		
$\widehat{u}$	($a/8$, $b/4$)	0.01879	0.01888	0.01889	**0.01887**	0.01887	0.01887	0.01916
	($a/4$, $b/8$)	0.01242	0.01244	**0.01244**	0.01244	0.01244	0.01242	0.01279
	($a/4$, $3b/8$)	0.03675	0.03678	**0.03678**	0.03678	0.03678	0.03678	0.03701
	($3a/8$, $b/4$)	−0.007547	−0.007557	−0.007553	**−0.007554**	−0.007554	−0.007554	−0.007446
$\widehat{v}$	($a/8$, $b/4$)	−0.02997	−0.02996	**−0.02996**	−0.02996	−0.02996	−0.02998	−0.02991
	($a/4$, $b/8$)	0.3516	0.3528	0.3530	**0.3529**	0.3529	0.3528	0.3547
	($a/4$, $3b/8$)	−0.05793	−0.05830	−0.05834	**−0.05832**	−0.05832	−0.05831	−0.05840
	($3a/8$, $b/4$)	−0.07325	−0.07319	**−0.07318**	−0.07318	−0.07318	−0.07327	−0.07322
$\widehat{w}$	($a/8$, $b/4$)	9.626	9.628	**9.629**	9.629	9.629	9.629	9.638
	($a/4$, $b/8$)	12.54	12.55	**12.55**	12.55	12.55	12.55	12.56
	($a/4$, $3b/8$)	8.486	8.488	**8.487**	8.487	8.487	8.487	8.488
	($3a/8$, $b/4$)	11.44	11.45	**11.45**	11.45	11.45	11.45	11.46

Table 2
Convergence for the bending moment solutions of CCCC cylindrical shell panels.

Displacement	Location	Number of series terms					SSM	FEM
		500	1000	1500	2000	2500		
$\overline{M}_1$	($a/8$, $b/4$)	−0.358	−0.356	−0.356	**−0.355**	−0.355	−0.354	−0.355
	($a/4$, $b/8$)	0.424	0.454	0.461	**0.471**	0.471	0.480	0.480
	($a/4$, $3b/8$)	−0.0981	−0.0710	−0.0650	**−0.0559**	−0.0559	−0.0485	−0.0485
	($3a/8$, $b/4$)	0.0359	0.0373	0.0376	**0.0380**	0.0380	0.0382	0.0376
$\overline{M}_2$	($a/8$, $b/4$)	−0.348	−0.340	−0.339	**−0.336**	−0.336	−0.334	−0.344
	($a/4$, $b/8$)	1.54	1.55	1.56	**1.56**	1.56	1.56	1.55
	($a/4$, $3b/8$)	−0.157	−0.148	−0.147	**−0.144**	−0.144	−0.142	−0.150
	($3a/8$, $b/4$)	0.0134	0.0178	0.0187	**0.0202**	0.0202	0.0211	0.0100

Table 3
Displacement solutions of CCCC cylindrical shell panels.

		$\widehat{u}$				$\widehat{v}$				$\widehat{w}$			
α	β	$b/8$	$b/4$	$3b/8$	$b/2$	$b/8$	$b/4$	$3b/8$	$b/2$	$b/8$	$b/4$	$3b/8$	$b/2$
$a/8$	FEM	0.01827	0.01916	0.05407	0.05937	0.2150	−0.02991	−0.02154	0	12.56	9.638	8.954	9.022
	SSM	0.01779	0.01887	0.05374	0.05906	0.2133	−0.02998	−0.02145	0	12.54	9.629	8.953	9.019
	Present	0.01782	0.01887	0.05374	0.05906	0.2134	−0.02996	−0.02145	0	12.54	9.629	8.953	9.019
$a/4$	FEM	0.01279	−0.005491	0.03701	0.04541	0.3547	−0.06310	−0.05840	0	12.56	10.57	8.488	8.835
	SSM	0.01242	−0.005698	0.03678	0.04521	0.3528	−0.06314	−0.05831	0	12.55	10.56	8.487	8.831
	Present	0.01244	−0.005698	0.03678	0.04521	0.3529	−0.06308	−0.05832	0	12.55	10.56	8.487	8.831
$3a/8$	FEM	0.006173	−0.007446	0.01809	0.02505	0.4218	−0.07322	−0.09432	0	12.20	11.46	8.140	8.670
	SSM	0.005984	−0.007554	0.01797	0.02495	0.4199	−0.07327	−0.09422	0	12.18	11.45	8.140	8.665
	Present	0.005995	−0.007554	0.01797	0.02495	0.4200	−0.07318	−0.09424	0	12.18	11.45	8.140	8.665
$a/2$	FEM	0	0	0	0	0.4417	−0.07427	−0.1090	0	12.05	11.78	8.025	8.590
	SSM	0	0	0	0	0.4399	−0.07432	−0.1089	0	12.04	11.77	8.026	8.586
	Present	0	0	0	0	0.4400	−0.07422	−0.1089	0	12.04	11.77	8.026	8.585

$$F_{T1} = \frac{E\delta}{1-\mu^2}\left[\frac{\partial u}{\partial \alpha} + \mu\left(\frac{\partial v}{\partial \beta} + \frac{w}{R}\right)\right] \tag{4}$$

$$F_{T2} = \frac{E\delta}{1-\mu^2}\left(\frac{\partial v}{\partial \beta} + \frac{w}{R} + \mu\frac{\partial u}{\partial \alpha}\right) \tag{5}$$

$$F_{T12} = \frac{E\delta}{2(1+\mu)}\left(\frac{\partial u}{\partial \beta} + \frac{\partial v}{\partial \alpha}\right) \tag{6}$$

$$M_1 = -\frac{E\delta^3}{12(1-\mu^2)}\left(\frac{\partial^2 w}{\partial \alpha^2} + \mu\frac{\partial^2 w}{\partial \beta^2}\right) \tag{7}$$

$$M_2 = -\frac{E\delta^3}{12(1-\mu^2)}\left(\frac{\partial^2 w}{\partial \beta^2} + \mu\frac{\partial^2 w}{\partial \alpha^2}\right) \tag{8}$$

$$M_{12} = -\frac{E\delta^3}{12(1+\mu)}\left(\frac{\partial^2 w}{\partial \alpha \partial \beta}\right) \tag{9}$$

$$F_{S1} = -\frac{E\delta^3}{12(1-\mu^2)}\frac{\partial}{\partial \alpha}\nabla^2 w \tag{10}$$

$$F_{S2} = -\frac{E\delta^3}{12(1-\mu^2)}\frac{\partial}{\partial \beta}\nabla^2 w \tag{11}$$

where F_{T1} and F_{T2} are the in-plane forces that are normal to the $o\beta$ and $o\alpha$ edges; F_{T12} is the in-plane shear force; F_{S1} and F_{S2} are the transverse shear forces in the cross sections that are perpendicular to the $o\alpha$ and $o\beta$ edges; M_1 and M_2 are the bending moments about the $o\beta$ and $o\alpha$ edges; M_{12} is the twisting moment.

Table 4
Displacement solutions of CCCS cylindrical shell panels.

		$\widehat{u}$				$\widehat{v}$				$\widehat{w}$			
α	β	$b/8$	$b/4$	$3b/8$	$b/2$	$b/8$	$b/4$	$3b/8$	$b/2$	$b/8$	$b/4$	$3b/8$	$b/2$
$a/8$	FEM	0.5367	1.055	1.427	1.522	0.004785	−0.3555	−0.1474	0	15.43	9.317	8.141	9.119
	SSM	0.5407	1.057	1.429	1.524	0.003268	−0.3552	−0.1475	0	15.43	9.287	8.133	9.110
	Present	0.5343	1.052	1.425	1.520	0.003474	−0.3552	−0.1476	0	15.43	9.288	8.133	9.109
$a/4$	FEM	0.4032	0.7872	1.101	1.188	0.01070	−0.6137	−0.2809	0	16.99	9.775	6.513	8.374
	SSM	0.3986	0.7827	1.097	1.184	0.008871	−0.6133	−0.2811	0	17.00	9.746	6.505	8.363
	Present	0.3986	0.7826	1.097	1.184	0.009131	−0.6132	−0.2812	0	16.99	9.749	6.505	8.362
$3a/8$	FEM	0.3118	0.5837	0.8074	0.8788	0.02697	−0.7422	−0.3749	0	17.44	10.48	5.464	7.769
	SSM	0.3086	0.5799	0.8038	0.8753	0.02538	−0.7416	−0.3752	0	17.29	10.85	5.197	7.459
	Present	0.3086	0.5798	0.8037	0.8752	0.02565	−0.7415	−0.3753	0	17.44	10.46	5.456	7.755
$a/2$	FEM	0.2440	0.4256	0.5499	0.5996	0.05502	−0.7533	−0.4038	0	17.31	10.84	5.188	7.465
	SSM	0.2457	0.4243	0.5515	0.6011	0.05369	−0.7525	−0.4040	0	17.28	10.84	5.191	7.445
	Present	0.2434	0.4243	0.5484	0.5981	0.05395	−0.7523	−0.4041	0	17.28	10.84	5.191	7.444
$5a/8$	FEM	0.1899	0.2991	0.3327	0.3613	0.08441	−0.6641	−0.3600	0	16.75	10.68	5.683	7.522
	SSM	0.1909	0.3003	0.3341	0.3625	0.08324	−0.6631	−0.3599	0	16.73	10.67	5.680	7.510
	Present	0.1895	0.2983	0.3317	0.3601	0.08347	−0.6629	−0.3600	0	16.73	10.67	5.680	7.508
$3a/4$	FEM	0.1368	0.1850	0.1559	0.1700	0.09871	−0.4880	−0.2583	0	15.88	10.01	6.801	7.885
	SSM	0.1361	0.1839	0.1544	0.1684	0.09765	−0.4868	−0.2579	0	15.85	10.01	6.801	7.877
	Present	0.1360	0.1839	0.1544	0.1683	0.09785	−0.4867	−0.2580	0	15.85	10.01	6.801	7.876
$7a/8$	FEM	0.07198	0.06260	0.02122	0.02653	0.07049	−0.2426	−0.1297	0	14.27	9.434	8.213	8.496
	SSM	0.07182	0.06218	0.02062	0.02579	0.06966	−0.2413	−0.1290	0	14.24	9.427	8.214	8.493
	Present	0.07178	0.06218	0.02061	0.02576	0.06980	−0.2413	−0.1291	0	14.24	9.428	8.214	8.493

Table 5
Displacement solutions of SCCC cylindrical shell panels.

		$\widehat{u}$				$\widehat{v}$				$\widehat{w}$			
β	α	$a/8$	$a/4$	$3a/8$	$a/2$	$a/8$	$a/4$	$3a/8$	$a/2$	$a/8$	$a/4$	$3a/8$	$a/2$
$b/8$	FEM	−4.505	−5.109	−3.145	0	3.948	6.936	9.122	9.930	160.0	318.5	433.2	474.1
	SSM	−4.489	−5.098	−3.139	0	3.872	6.818	8.978	9.776	158.2	315.6	429.7	470.5
	Present	−4.485	−5.095	−3.138	0	3.873	6.817	8.976	9.774	158.1	315.4	429.5	470.3
$b/4$	FEM	−0.6031	−0.8748	−0.6208	0	−3.188	−8.580	−13.10	−14.83	−0.02856	−26.78	−45.23	−51.23
	SSM	−0.6016	−0.8718	−0.6186	0	−3.165	−8.525	−13.03	−14.74	−0.01682	−26.64	−45.09	−51.10
	Present	−0.6003	−0.8705	−0.6179	0	−3.159	−8.517	−13.02	−14.73	0.01230	−26.62	−45.09	−51.10
$3b/8$	FEM	0.7632	0.9285	0.6080	0	−0.1739	−0.09141	−0.01389	0.006368	−12.06	−42.68	−70.26	−81.3
	SSM	0.7578	0.9223	0.6041	0	−0.1747	−0.09869	−0.02543	−0.006495	−11.89	−42.30	−69.70	−80.66
	Present	0.7570	0.9218	0.6038	0	−0.1745	−0.09762	−0.02356	−0.004294	−11.86	−42.24	−69.62	−80.58
$b/2$	FEM	0.03008	0.007910	0.000025	0	0.5848	1.510	2.312	2.628	13.54	23.21	32.23	35.84
	SSM	0.03136	0.009612	0.001141	0	0.5794	1.498	2.295	2.608	13.48	23.02	31.93	35.50
	Present	0.03122	0.009414	0.001006	0	0.5785	1.496	2.292	2.605	13.47	23.02	31.93	35.50
$5b/8$	FEM	−0.07478	−0.1223	−0.08620	0	−0.04839	−0.2062	−0.3561	−0.4168	12.18	15.34	17.9	18.89
	SSM	−0.07419	−0.1214	−0.08562	0	−0.04669	−0.2006	−0.3472	−0.4065	12.15	15.31	17.86	18.85
	Present	−0.07399	−0.1213	−0.08553	0	−0.04664	−0.2006	−0.3472	−0.4066	12.14	15.30	17.85	18.83
$3b/4$	FEM	0.04358	0.02503	0.01274	0	−0.06726	−0.1634	−0.2569	−0.2949	8.281	6.788	5.534	5.015
	SSM	0.04266	0.02407	0.01214	0	−0.06633	−0.1620	−0.2552	−0.2931	8.293	6.831	5.603	5.094
	Present	0.04268	0.02409	0.01215	0	−0.06626	−0.1618	−0.2550	−0.2929	8.298	6.838	5.612	5.103
$7b/8$	FEM	0.03169	0.02906	0.01666	0	−0.2070	−0.3152	−0.3524	−0.3605	12.42	12.51	12.28	12.19
	SSM	0.03115	0.02862	0.01643	0	−0.2056	−0.3145	−0.3522	−0.3605	12.40	12.48	12.24	12.15
	Present	0.03123	0.02867	0.01645	0	−0.2060	−0.3149	−0.3527	−0.3610	12.40	12.48	12.24	12.15

The non-Lévy-type cylindrical shell panels without a free edge include CCCC, CCCS, SCCC and SCCS cases, which will be treated successively in the following.

2.2. Double finite integral transforms

Three pairs of double finite integral transforms with respect to u, v, and w are defined. The transforms are

$$\begin{aligned}
\overline{u}_{\mathrm{cs}}(m,n) &= \int_0^a \int_0^b u(x,y)\cos(\lambda_m\alpha)\sin(\gamma_n\beta)\mathrm{d}\alpha\mathrm{d}\beta \\
\overline{v}_{\mathrm{sc}}(m,n) &= \int_0^a \int_0^b v(x,y)\sin(\lambda_m\alpha)\cos(\gamma_n\beta)\mathrm{d}\alpha\mathrm{d}\beta \\
\overline{w}_{\mathrm{ss}}(m,n) &= \int_0^a \int_0^b w(x,y)\sin(\lambda_m\alpha)\sin(\gamma_n\beta)\mathrm{d}\alpha d\beta
\end{aligned} \tag{12}$$

and the inversions are

$$\begin{aligned}
u(\alpha,\beta) &= \frac{2}{ab}\sum_{m=0}^{\infty}\sum_{n=1}^{\infty}\varepsilon_m\overline{u}_{\mathrm{cs}}(m,n)\cos(\lambda_m\alpha)\sin(\gamma_n\beta) \\
v(\alpha,\beta) &= \frac{2}{ab}\sum_{m=1}^{\infty}\sum_{n=0}^{\infty}\varepsilon_n\overline{v}_{\mathrm{sc}}(m,n)\sin(\lambda_m\alpha)\cos(\gamma_n\beta) \\
w(\alpha,\beta) &= \frac{4}{ab}\sum_{m=1}^{\infty}\sum_{n=1}^{\infty}\overline{w}_{\mathrm{ss}}(m,n)\sin(\lambda_m\alpha)\sin(\gamma_n\beta)
\end{aligned} \tag{13}$$

where $\lambda_m = m\pi/a$, $\gamma_n = n\pi/b$, $\varepsilon_m = \begin{cases} 1 & \text{for } m = 0 \\ 2 & \text{for } m = 1,2,3,\cdots \end{cases}$, and $\varepsilon_n = \begin{cases} 1 & \text{for } n = 0 \\ 2 & \text{for } n = 1,2,3,\cdots \end{cases}$.

Table 6
Longitudinal displacement solutions, $\widehat{u}$, of SCCS cylindrical shell panels.

α	β	0	$b/8$	$b/4$	$3b/8$	$b/2$	$5b/8$	$3b/4$	$7b/8$
0	FEM	0	−14.22	−4.685	2.204	1.33	0.5061	0.8215	0.6284
	SSM	0	−14.17	−4.683	2.192	1.338	0.5117	0.8185	0.6243
	Present	0	−14.17	−4.682	2.191	1.337	0.5115	0.8183	0.6243
$a/8$	FEM	0	−12.89	−4.637	1.695	0.9637	0.2501	0.5308	0.4113
	SSM	0	−12.84	−4.633	1.685	0.9709	0.2555	0.5284	0.4077
	Present	0	−12.84	−4.632	1.684	0.9701	0.2553	0.5283	0.4078
$a/4$	FEM	0	−9.104	−3.838	0.8433	0.5219	0.1098	0.3075	0.2621
	SSM	0	−9.067	−3.832	0.8377	0.5275	0.1140	0.3061	0.2596
	Present	0	−9.065	−3.832	0.8368	0.5269	0.1139	0.3059	0.2596
$3a/8$	FEM	0	−4.185	−2.394	−0.1874	0.08433	0.08704	0.1733	0.1552
	SSM	0	−4.165	−2.386	−0.1867	0.08761	0.08939	0.1730	0.1539
	Present	0	−4.164	−2.386	−0.1875	0.08720	0.08928	0.1729	0.1539
$a/2$	FEM	0	0.7792	−0.7171	−1.173	−0.2884	0.1303	0.09980	0.07683
	SSM	0	0.7822	−0.7068	−1.166	−0.2877	0.1306	0.1006	0.07647
	Present	0	0.7828	−0.7072	−1.167	−0.2878	0.1305	0.1005	0.07645
$5a/8$	FEM	0	4.830	0.6653	−1.849	−0.5305	0.1780	0.06142	0.02073
	SSM	0	4.819	0.6761	−1.838	−0.5318	0.1767	0.06297	0.02111
	Present	0	4.818	0.6752	−1.838	−0.5317	0.1766	0.06291	0.02106
$3a/4$	FEM	0	6.920	1.307	−1.973	−0.5896	0.1775	0.03389	−0.01481
	SSM	0	6.900	1.316	−1.960	−0.5918	0.1754	0.03572	−0.01395
	Present	0	6.898	1.315	−1.959	−0.5915	0.1753	0.03566	−0.01403
$7a/8$	FEM	0	5.730	1.018	−1.383	−0.4357	0.09827	−0.007010	−0.02864
	SSM	0	5.711	1.024	−1.373	−0.4372	0.09669	−0.005571	−0.02773
	Present	0	5.707	1.022	−1.372	−0.4368	0.09654	−0.005620	−0.02783

Table 7
Circumferential displacement solutions, $\widehat{v}$, of SCCS cylindrical shell panels.

α	β	0	$b/8$	$b/4$	$3b/8$	$b/2$	$5b/8$	$3b/4$	$7b/8$
0	FEM	0	0	0	0	0	0	0	0
	SSM	0	0	0	0	0	0	0	0
	Present	0	0	0	0	0	0	0	0
$a/8$	FEM	35.25	4.444	−11.34	−1.787	2.172	0.1622	−0.2303	−0.08377
	SSM	35.14	4.442	−11.29	−1.806	2.156	0.1721	−0.2261	−0.08346
	Present	35.13	4.441	−11.29	−1.805	2.155	0.1717	−0.2260	−0.08420
$a/4$	FEM	59.82	8.951	−20.31	−3.294	3.883	0.2942	−0.4430	−0.1602
	SSM	59.61	8.921	−20.22	−3.330	3.854	0.3118	−0.4354	−0.1604
	Present	59.60	8.919	−20.21	−3.327	3.853	0.3112	−0.4354	−0.1613
$3a/8$	FEM	72.89	12.16	−25.07	−4.239	4.760	0.3693	−0.5840	−0.2310
	SSM	72.63	12.10	−24.95	−4.283	4.725	0.3910	−0.5739	−0.2317
	Present	72.62	12.09	−24.95	−4.280	4.723	0.3903	−0.5739	−0.2326
$a/2$	FEM	74.52	13.21	−24.92	−4.400	4.620	0.3759	−0.5984	−0.2912
	SSM	74.24	13.13	−24.81	−4.441	4.584	0.3973	−0.5884	−0.2919
	Present	74.22	13.12	−24.80	−4.439	4.582	0.3965	−0.5885	−0.2927
$5a/8$	FEM	65.49	11.96	−20.30	−3.7900	3.571	0.3192	−0.4831	−0.3250
	SSM	65.23	11.89	−20.20	−3.819	3.542	0.3363	−0.4744	−0.3250
	Present	65.22	11.89	−20.19	−3.817	3.540	0.3357	−0.4745	−0.3257
$3a/4$	FEM	47.54	8.905	−12.67	−2.674	2.029	0.2164	−0.2877	−0.3096
	SSM	47.33	8.846	−12.60	−2.686	2.011	0.2268	−0.2816	−0.3086
	Present	47.31	8.845	−12.59	−2.684	2.009	0.2263	−0.2816	−0.3092
$7a/8$	FEM	23.72	4.889	−4.657	−1.361	0.6045	0.09829	−0.1026	−0.2073
	SSM	23.56	4.839	−4.625	−1.357	0.5987	0.1019	−0.09953	−0.2056
	Present	23.55	4.840	−4.619	−1.357	0.5974	0.1016	−0.09953	−0.2060

2.3. Solution procedure with applications to fully clamped cylindrical shell panels

Applying the three transforms in Eq. (12) over Eqs. (1)–(3), respectively, we obtain

$$\int_0^b \left[\frac{\partial u}{\partial \alpha}\cos(\lambda_m\alpha)\right]\Big|_0^a \sin(\gamma_n\beta)\mathrm{d}\beta - \frac{1-\mu}{2}\gamma_n\int_0^b [u\cos(\lambda_m\alpha)]|_0^a \cos(\gamma_n\beta)\mathrm{d}\beta$$
$$-\left(\lambda_m^2+\frac{1-\mu}{2}\gamma_n^2\right)\overline{u}_{\mathrm{cs}} - \frac{1+\mu}{2}\left\{\gamma_n\int_0^b [v\cos(\lambda_m\alpha)]|_0^a \cos(\gamma_n\beta)\mathrm{d}\beta + \lambda_m\gamma_n\overline{v}_{\mathrm{sc}}\right\}$$
$$+\frac{\mu}{R}\left\{\int_0^b [w\cos(\lambda_m\alpha)]|_0^a \sin(\gamma_n\beta)\mathrm{d}\beta + \lambda_m\overline{w}_{\mathrm{ss}}\right\} = -\frac{1-\mu^2}{E\delta}\overline{q}_{1\mathrm{cs}} \tag{14}$$

$$\int_0^a \left[\frac{\partial v}{\partial \beta}\cos(\gamma_n\beta)\right]\Big|_0^b \sin(\lambda_m\alpha)\mathrm{d}\alpha - \frac{1-\mu}{2}\lambda_m\int_0^a [v\cos(\gamma_n\beta)]|_0^b \cos(\lambda_m\alpha)\mathrm{d}\alpha$$
$$-\frac{1+\mu}{2}\left\{\lambda_m\int_0^a [u\cos(\gamma_n\beta)]|_0^b \cos(\lambda_m\alpha)\mathrm{d}\alpha + \lambda_m\gamma_n\overline{u}_{\mathrm{cs}}\right\} - \left(\frac{1-\mu}{2}\lambda_m^2+\gamma_n^2\right)\overline{v}_{\mathrm{sc}}$$
$$+\frac{1}{R}\left\{\int_0^a [w\cos(\gamma_n\beta)]|_0^b \sin(\lambda_m\alpha)\mathrm{d}\alpha + \gamma_n\overline{w}_{\mathrm{ss}}\right\} = -\frac{1-\mu^2}{E\delta}\overline{q}_{2\mathrm{sc}} \tag{15}$$

Table 8
Radial displacement solutions, $\widehat{w}$, of SCCS cylindrical shell panels.

α	β	0	$b/8$	$b/4$	$3b/8$	$b/2$	$5b/8$	$3b/4$	$7b/8$
0	FEM	0	0	0	0	0	0	0	0
	SSM	0	0	0	0	0	0	0	0
	Present	0	0	0	0	0	0	0	0
$a/8$	FEM	0	294.2	−19.16	−64.26	16.39	23.02	5.952	13.04
	SSM	0	293.0	−18.71	−63.91	16.13	22.95	6.036	13.01
	Present	0	293.0	−18.72	−63.89	16.13	22.94	6.039	13.02
$a/4$	FEM	0	507.8	−34.45	−125.0	21.59	33.04	3.821	12.62
	SSM	0	505.7	−33.65	−124.3	21.12	32.92	3.971	12.59
	Present	0	505.6	−33.67	−124.3	21.13	32.91	3.977	12.59
$3a/8$	FEM	0	620.9	−36.14	−159.1	24.03	38.00	3.274	11.81
	SSM	0	618.2	−35.18	−158.3	23.46	37.86	3.459	11.78
	Present	0	618.1	−35.19	−158.2	23.47	37.84	3.466	11.77
$a/2$	FEM	0	629.9	−31.26	−158.7	22.76	37.16	3.984	11.31
	SSM	0	627.1	−30.34	−157.9	22.19	37.02	4.167	11.28
	Present	0	627.0	−30.35	−157.8	22.20	37.00	4.174	11.28
$5a/8$	FEM	0	543.8	−22.82	−126.1	18.05	31.26	5.522	11.33
	SSM	0	541.3	−22.11	−125.4	17.61	31.13	5.667	11.32
	Present	0	541.1	−22.10	−125.4	17.61	31.12	5.674	11.31
$3a/4$	FEM	0	382.5	−8.702	−74.49	11.77	22.54	7.230	11.85
	SSM	0	380.6	−8.322	−74.00	11.52	22.44	7.316	11.83
	Present	0	380.5	−8.303	−73.95	11.51	22.43	7.322	11.83
$7a/8$	FEM	0	185.6	9.953	−23.82	7.156	14.14	8.664	12.17
	SSM	0	184.4	9.981	−23.57	7.090	14.10	8.691	12.16
	Present	0	184.3	10.01	−23.54	7.087	14.09	8.695	12.16

Table 9
Bending moment solutions of CCCC cylindrical shell panels.

		$\widehat{M}_1$					$\widehat{M}_2$				
α	β	0	$b/8$	$b/4$	$3b/8$	$b/2$	0	$b/8$	$b/4$	$3b/8$	$b/2$
0	FEM	0.719	−30.9	−27.9	−27.4	−27.3	0.715	−9.32	−8.42	−8.26	−8.23
	SSM	0	−31.1	−28.1	−27.6	−27.5	0	−9.32	−8.43	−8.28	−8.25
	Present	0	−31.1	−28.2	−27.6	−27.6	0	−9.34	−8.45	−8.29	−8.27
$a/8$	FEM	−2.52	0.393	−0.355	−0.216	−0.215	−8.39	1.37	−0.344	−0.0988	−0.0572
	SSM	−2.52	0.393	−0.354	−0.216	−0.216	−8.38	1.38	−0.334	−0.0901	−0.0512
	Present	−2.52	0.393	−0.355	−0.216	−0.216	−8.39	1.38	−0.336	−0.0901	−0.0495
$a/4$	FEM	−1.62	0.480	−0.0554	−0.0485	0.0259	−5.40	1.55	−0.219	−0.150	0.0738
	SSM	−1.61	0.480	−0.0548	−0.0485	0.0248	−5.38	1.56	−0.209	−0.142	0.0791
	Present	−1.62	0.471	−0.0627	−0.0559	0.0177	−5.38	1.56	−0.212	−0.144	0.0778
$3a/8$	FEM	−1.33	0.391	0.0376	−0.100	0.0407	−4.45	1.34	0.0100	−0.296	0.143
	SSM	−1.33	0.391	0.0382	−0.0993	0.0394	−4.43	1.35	0.0211	−0.287	0.147
	Present	−1.33	0.391	0.0380	−0.0992	0.0398	−4.43	1.35	0.0202	−0.287	0.148
$a/2$	FEM	−1.26	0.365	0.0678	−0.115	0.0436	−4.20	1.26	0.102	−0.353	0.168
	SSM	−1.25	0.365	0.0684	−0.115	0.0422	−4.18	1.27	0.113	−0.343	0.172
	Present	−1.25	0.371	0.0737	−0.110	0.0478	−4.18	1.27	0.114	−0.342	0.175

$$
\begin{aligned}
&-\frac{\mu}{R}\lambda_m\overline{u}_{\mathrm{cs}}-\frac{\gamma_n}{R}\overline{v}_{\mathrm{sc}}+\left[\frac{1}{R^2}+\frac{\delta^2}{12}\left(\lambda_m^2+\gamma_n^2\right)^2\right]\overline{w}_{\mathrm{ss}}\\
&+\frac{\delta^2}{12}\left\{\lambda_m^3\int_0^b[w\cos(\lambda_m\alpha)]|_0^a\sin(\gamma_n\beta)\mathrm{d}\beta+\lambda_m^2\gamma_n\int_0^a[w\cos(\gamma_n\beta)]|_0^b\sin(\lambda_m\alpha)\mathrm{d}\alpha\right.\\
&\left.+\lambda_m\gamma_n^2\int_0^b[w\cos(\lambda_m\alpha)]|_0^a\sin(\gamma_n\beta)\mathrm{d}\beta+\gamma_n^3\int_0^a[w\cos(\gamma_n\beta)]|_0^b\sin(\lambda_m\alpha)\mathrm{d}\alpha\right\}\\
&-\frac{\delta^2}{12}\left\{\lambda_m\int_0^b\left[\frac{\partial^2 w}{\partial\alpha^2}\cos(\lambda_m\alpha)\right]\Big|_0^a\sin(\gamma_n\beta)\mathrm{d}\beta+\gamma_n\int_0^a\left[\frac{\partial^2 w}{\partial\beta^2}\cos(\gamma_n\beta)\right]\Big|_0^b\sin(\lambda_m\alpha)\mathrm{d}\alpha\right\}\\
&\frac{1-\mu^2}{E\delta}\overline{q}_{3\mathrm{ss}}
\end{aligned}
\tag{16}
$$

where $\overline{q}_{1\mathrm{cs}}$, $\overline{q}_{2\mathrm{sc}}$, and $\overline{q}_{3\mathrm{ss}}$ are the transforms of the external load components as defined for those of u, v, and w in Eq. (12).

Without loss of generality, we first focus on CCCC panels. The boundary conditions are

$$
\begin{aligned}
&\left(u,v,w,\frac{\partial w}{\partial\alpha}\right)\Big|_{\alpha=0}=0\\
&\left(u,v,w,\frac{\partial w}{\partial\alpha}\right)\Big|_{\alpha=a}=0\\
&\left(u,v,w,\frac{\partial w}{\partial\beta}\right)\Big|_{\beta=0}=0\\
&\left(u,v,w,\frac{\partial w}{\partial\beta}\right)\Big|_{\beta=b}=0
\end{aligned}
\tag{17}
$$

Substituting the boundary conditions $v|_{\alpha=0,a}=0$, $u|_{\beta=0,b}=0$, $w|_{\alpha=0,a}=0$, and $w|_{\beta=0,b}=0$ into Eqs. (14)–(16) yields

$$
\begin{aligned}
&\int_0^b\left[\frac{\partial u}{\partial\alpha}\cos(\lambda_m\alpha)\right]\Big|_0^a\sin(\gamma_n\beta)\mathrm{d}\beta-\left(\lambda_m^2+\frac{1-\mu}{2}\gamma_n^2\right)\overline{u}_{\mathrm{cs}}\\
&-\frac{1+\mu}{2}\lambda_m\gamma_n\overline{v}_{\mathrm{sc}}+\frac{\mu}{R}\lambda_m\overline{w}_{\mathrm{ss}}=-\frac{1-\mu^2}{E\delta}\overline{q}_{1\mathrm{cs}}
\end{aligned}
\tag{18}
$$

Table 10
Bending moment solutions of CCCS cylindrical shell panels.

		$\widehat{M}_1$					$\widehat{M}_2$				
α	β	0	$b/8$	$b/4$	$3b/8$	$b/2$	0	$b/8$	$b/4$	$3b/8$	$b/2$
0	FEM	−1.14	0.148	0.178	0.183	0.184	1.87	0.00511	0.0294	0.0330	0.0340
	SSM	0	0	0	0	0	0	0	0	0	0
	Present	0	0	0	0	0	0	0	0	0	0
$a/8$	FEM	−3.25	0.611	−0.408	−0.218	−0.130	−10.8	1.98	−0.602	−0.173	0.106
	SSM	−3.26	0.613	−0.410	−0.218	−0.132	−10.9	1.99	−0.595	−0.165	0.111
	Present	−3.26	0.617	−0.407	−0.215	−0.129	−10.9	1.99	−0.597	−0.164	0.114
$a/4$	FEM	−2.66	0.791	−0.193	−0.130	0.0930	−8.86	2.46	−0.614	−0.328	0.331
	SSM	−2.66	0.794	−0.195	−0.131	0.0910	−8.87	2.47	−0.608	−0.320	0.334
	Present	−2.66	0.793	−0.197	−0.132	0.0907	−8.88	2.47	−0.611	−0.321	0.335
$3a/8$	FEM	−2.41	0.770	−0.112	−0.198	0.122	−8.02	2.46	−0.445	−0.527	0.451
	SSM	−2.41	0.772	−0.112	−0.199	0.120	−8.02	2.47	−0.437	−0.521	0.454
	Present	−2.41	0.769	−0.115	−0.202	0.118	−8.02	2.47	−0.439	−0.522	0.454
$a/2$	FEM	−2.26	0.738	−0.0694	−0.215	0.121	−7.54	2.38	−0.339	−0.590	0.465
	SSM	−2.26	0.739	−0.0686	−0.216	0.119	−7.53	2.39	−0.329	−0.584	0.468
	Present	−2.26	0.742	−0.0662	−0.213	0.122	−7.54	2.40	−0.329	−0.584	0.470
$5a/8$	FEM	−2.22	0.711	−0.0797	−0.179	0.0985	−7.40	2.31	−0.369	−0.488	0.373
	SSM	−2.22	0.711	−0.0786	−0.180	0.0964	−7.38	2.32	−0.358	−0.482	0.375
	Present	−2.22	0.720	−0.0800	−0.180	0.100	−7.39	2.32	−0.358	−0.481	0.377
$3a/4$	FEM	−2.36	0.708	−0.146	−0.0919	0.0526	−7.85	2.24	−0.495	−0.263	0.203
	SSM	−2.35	0.707	−0.144	−0.0925	0.0508	−7.83	2.25	−0.483	−0.257	0.206
	Present	−2.35	0.700	−0.152	−0.0988	0.0449	−7.84	2.25	−0.487	−0.259	0.206
$7a/8$	FEM	−3.06	0.473	−0.400	−0.228	−0.220	−10.2	1.66	−0.466	−0.142	−0.0199
	SSM	−3.06	0.472	−0.399	−0.228	−0.221	−10.2	1.67	−0.455	−0.134	−0.0149
	Present	−3.06	0.470	−0.402	−0.230	−0.222	−10.2	1.67	−0.458	−0.135	−0.0138
a	FEM	0.687	−32.4	−28.3	−27.3	−27.3	0.684	−9.76	−8.53	−8.23	−8.22
	SSM	0	−32.6	−28.4	−27.5	−27.5	0	−9.69	−8.61	−8.25	−8.21
	Present	0	−32.6	−28.5	−27.6	−27.6	0	−9.77	−8.56	−8.27	−8.27

Table 11
Bending moment solutions of SCCC cylindrical shell panels.

		$\widehat{M}_1$					$\widehat{M}_2$				
β	α	0	$a/8$	$a/4$	$3a/8$	$a/2$	0	$a/8$	$a/4$	$3a/8$	$a/2$
0	FEM	16.5	−0.209	−0.160	−0.145	−0.141	−10.1	−0.0830	0	0.0335	0.0419
	SSM	0	0	0	0	0	0	0	0	0	0
	Present	0	0	0	0	0	0	0	0	0	0
$b/8$	FEM	−136	2.64	14.9	22.5	25.1	−41.1	14.1	41.4	61.7	68.9
	SSM	−134	2.62	14.8	22.5	25.0	−40.3	14.0	41.2	61.5	68.7
	Present	−135	2.61	14.7	22.4	25.1	−40.6	14.0	41.1	61.5	68.7
$b/4$	FEM	−37.5	−3.01	−8.81	−12.5	−13.7	−11.4	−11.1	−27.6	−39.6	−43.6
	SSM	−37.4	−2.96	−8.73	−12.5	−13.6	−11.2	−11.0	−27.4	−39.3	−43.3
	Present	−37.8	−2.96	−8.76	−12.5	−13.6	−11.3	−11.0	−27.4	−39.3	−43.3
$3b/8$	FEM	−14.3	0.0292	−1.01	−2.36	−2.96	−4.31	−1.40	−2.83	−4.79	−5.78
	SSM	−14.7	0.0229	−1.01	−2.36	−2.96	−4.40	−1.40	−2.84	−4.81	−5.78
	Present	−14.8	0.0237	−1.02	−2.35	−2.94	−4.44	−1.40	−2.84	−4.79	−5.77
$b/2$	FEM	−27.8	0.109	1.70	2.96	3.47	−8.39	1.92	5.53	8.86	10.2
	SSM	−28.0	0.105	1.69	2.94	3.44	−8.41	1.91	5.49	8.79	10.1
	Present	−28.3	0.105	1.66	2.94	3.46	−8.48	1.91	5.48	8.79	10.1
$5b/8$	FEM	−29.8	−0.271	−0.120	−0.241	−0.293	−9.00	−0.114	−0.524	−1.10	−1.35
	SSM	−30.0	−0.269	−0.114	−0.232	−0.282	−9.00	−0.100	−0.498	−1.06	−1.30
	Present	−30.3	−0.270	−0.140	−0.233	−0.266	−9.08	−0.103	−0.508	−1.06	−1.30
$3b/4$	FEM	−27.5	−0.418	−0.372	−0.483	−0.529	−8.28	−0.745	−1.22	−1.48	−1.58
	SSM	−27.7	−0.417	−0.369	−0.479	−0.525	−8.30	−0.731	−1.20	−1.46	−1.56
	Present	−27.9	−0.419	−0.393	−0.479	−0.508	−8.37	−0.736	−1.21	−1.46	−1.55
$7b/8$	FEM	−30.6	0.429	0.609	0.604	0.611	−9.24	1.52	1.99	2.04	2.06
	SSM	−30.8	0.428	0.606	0.600	0.607	−9.24	1.52	1.99	2.03	2.05
	Present	−31.1	0.429	0.582	0.601	0.625	−9.24	1.52	1.99	2.03	2.06
b	FEM	0.720	−2.57	−1.80	−1.63	−1.59	0.715	−8.55	−5.99	−5.42	−5.32
	SSM	0	−2.57	−1.75	−1.63	−1.60	0	−8.53	−6.00	−5.39	−5.27
	Present	0	−2.57	−1.80	−1.62	−1.59	0	−8.58	−5.98	−5.41	−5.30

$$\int_0^a \left[\frac{\partial v}{\partial \beta}\cos(\gamma_n \beta)\right]\Big|_0^b \sin(\lambda_m \alpha)\mathrm{d}x - \frac{1+\mu}{2}\lambda_m \gamma_n \overline{u}_{\mathrm{cs}} - \left(\frac{1-\mu}{2}\lambda_m^2 + \gamma_n^2\right)\overline{v}_{\mathrm{sc}} + \frac{1}{R}\gamma_n \overline{w}_{\mathrm{ss}} = -\frac{1-\mu^2}{E\delta}\overline{q}_{2\mathrm{sc}} \tag{19}$$

Table 12
Bending moment solutions, $\widehat{M}_1$, of SCCS cylindrical shell panels.

		$\widehat{M}_1$								
α	β	0	$b/8$	$b/4$	$3b/8$	$b/2$	$5b/8$	$3b/4$	$7b/8$	b
0	FEM	0.0264	0.187	0.187	0.187	0.187	0.187	0.187	0.187	0.079
	SSM	0	0	0	0	0	0	0	0	0
	Present	0	0	0	0	0	0	0	0	0
$a/8$	FEM	0.0737	15.1	−7.72	−2.98	1.68	0.348	−0.908	0.617	−3.32
	SSM	0	15.1	−7.68	−3.00	1.66	0.353	−0.902	0.609	−3.23
	Present	0	15.1	−7.68	−3.00	1.66	0.352	−0.901	0.608	−3.32
$a/4$	FEM	0.0668	27.1	−12.6	−5.41	3.43	0.853	−1.08	0.787	−2.75
	SSM	0	27.1	−12.6	−5.43	3.39	0.863	−1.07	0.780	−2.78
	Present	0	27.1	−12.6	−5.43	3.40	0.863	−1.06	0.780	−2.75
$3a/8$	FEM	0.0634	32.6	−14.7	−7.07	4.35	0.969	−1.17	0.743	−2.45
	SSM	0	32.6	−14.5	−7.09	4.30	0.983	−1.16	0.735	−2.46
	Present	0	32.6	−14.5	−7.09	4.30	0.979	−1.16	0.732	−2.45
$a/2$	FEM	0.0632	32.4	−14.5	−6.98	4.29	0.898	−1.08	0.676	−2.21
	SSM	0	32.4	−14.4	−7.00	4.25	0.911	−1.07	0.668	−2.17
	Present	0	32.4	−14.4	−7.00	4.25	0.913	−1.06	0.670	−2.20
$5a/8$	FEM	0.0657	27.0	−12.6	−5.10	3.29	0.679	−0.835	0.612	−2.01
	SSM	0	27.0	−12.5	−5.11	3.25	0.689	−0.824	0.606	−2.00
	Present	0	26.9	−12.5	−5.11	3.25	0.683	−0.827	0.600	−2.01
$3a/4$	FEM	0.0706	16.8	−8.63	−2.31	1.74	0.368	−0.537	0.597	−2.00
	SSM	0	16.8	−8.57	−2.32	1.72	0.373	−0.531	0.593	−1.98
	Present	0	16.9	−8.55	−2.31	1.73	0.380	−0.522	0.600	−1.99
$7a/8$	FEM	0.0771	2.48	−2.94	0.0353	0.127	−0.231	−0.457	0.426	−2.64
	SSM	0	2.51	−2.91	0.0305	0.122	−0.229	−0.455	0.425	−2.64
	Present	0	2.42	−2.93	0.0273	0.109	−0.246	−0.469	0.408	−2.64
a	FEM	0.0258	−155	−46.7	−6.72	−21.3	−29.9	−28.0	−30.6	0.718
	SSM	0	−153	−46.5	−7.07	−21.6	−30.0	−28.1	−30.8	0
	Present	0	−155	−47.0	−7.16	−21.7	−30.3	−28.4	−31.0	0

Table 13
Bending moment solutions, $\widehat{M}_2$, of SCCS cylindrical shell panels.

		$\widehat{M}_2$								
α	β	0	$b/8$	$b/4$	$3b/8$	$b/2$	$5b/8$	$3b/4$	$7b/8$	b
0	FEM	0.0264	0.0796	0.0803	0.0803	0.0803	0.0803	0.0803	0.0803	0
	SSM	0	0	0	0	0	0	0	0	0
	Present	0	0	0	0	0	0	0	0	0
$a/8$	FEM	0.202	37.6	−22.5	−7.04	5.91	1.12	−2.13	2.06	−11.0
	SSM	0	37.6	−22.3	−7.07	5.86	1.15	−2.10	2.05	−11.1
	Present	0	37.6	−22.3	−7.07	5.86	1.15	−2.10	2.05	−11.1
$a/4$	FEM	0.204	72.0	−39.6	−13.2	10.9	1.93	−3.31	2.58	−9.15
	SSM	0	72.1	−39.4	−13.3	10.8	1.97	−3.27	2.56	−9.07
	Present	0	72.1	−39.4	−13.3	10.8	1.97	−3.27	2.56	−9.15
$3a/8$	FEM	0.205	90.0	−47.8	−17.3	13.8	2.17	−3.70	2.53	−8.17
	SSM	0	90.0	−47.4	−17.4	13.7	2.23	−3.65	2.51	−8.13
	Present	0	90.0	−47.4	−17.4	13.7	2.22	−3.65	2.51	−8.15
$a/2$	FEM	0.205	90.8	−47.9	−17.4	13.7	2.06	−3.46	2.34	−7.35
	SSM	0	90.9	−47.5	−17.5	13.5	2.12	−3.41	2.32	−7.32
	Present	0	90.8	−47.5	−17.5	13.5	2.11	−3.40	2.32	−7.32
$5a/8$	FEM	0.204	76.3	−41.1	−13.5	10.6	1.74	−2.76	2.12	−6.71
	SSM	0	76.3	−40.8	−13.6	10.5	1.78	−2.72	2.11	−6.68
	Present	0	76.3	−40.8	−13.5	10.5	1.78	−2.72	2.11	−6.69
$3a/4$	FEM	0.203	49.1	−27.7	−7.88	6.09	1.27	−1.86	1.98	−6.66
	SSM	0	49.2	−27.5	−7.91	6.03	1.30	−1.84	1.97	−6.63
	Present	0	49.2	−27.5	−7.90	6.03	1.29	−1.83	1.97	−6.65
$7a/8$	FEM	0.201	16.7	−10.8	−3.21	1.90	0.568	−0.907	1.48	−8.79
	SSM	0	16.8	−10.7	−3.20	1.87	0.580	−0.890	1.48	−8.78
	Present	0	16.7	−10.7	−3.20	1.87	0.572	−0.891	1.48	−8.81
a	FEM	0.194	−46.8	−14.1	−2.01	−6.41	−9.00	−8.43	−9.23	0.713
	SSM	0	−46.0	−14.0	−2.12	−6.47	−9.02	−8.48	−9.15	0
	Present	0	−46.3	−14.1	−2.15	−6.52	−9.08	−8.52	−9.30	0

$$-\frac{\mu}{R}\lambda_m\overline{u}_{\rm cs}-\frac{\gamma_n}{R}\overline{v}_{\rm sc}+\left[\frac{1}{R^2}+\frac{\delta^2}{12}\left(\lambda_m^2+\gamma_n^2\right)^2\right]\overline{w}_{\rm ss}$$
$$-\frac{\delta^2}{12}\left\{\lambda_m\int_0^b\left[\frac{\partial^2 w}{\partial\alpha^2}\cos(\lambda_m\alpha)\right]\Big|_0^a\sin(\gamma_n\beta)\mathrm{d}\beta\right.$$
$$\left.+\gamma_n\int_0^a\left[\frac{\partial^2 w}{\partial\beta^2}\cos(\gamma_n\beta)\right]\Big|_0^b\sin(\lambda_m\alpha)\mathrm{d}\alpha\right\}=\frac{1-\mu^2}{E\delta}\overline{q}_{\rm 3ss} \tag{20}$$

Denote

$$I_{na}=\int_0^b\frac{\partial^2 w}{\partial\alpha^2}\Big|_{\alpha=a}\sin(\gamma_n\beta)\mathrm{d}\beta,\quad I_{n0}=\int_0^b\frac{\partial^2 w}{\partial\alpha^2}\Big|_{\alpha=0}\sin(\gamma_n\beta)\mathrm{d}\beta$$
$$J_{mb}=\int_0^a\frac{\partial^2 w}{\partial\beta^2}\Big|_{\beta=b}\sin(\lambda_m\alpha)\mathrm{d}\alpha,\quad J_{m0}=\int_0^a\frac{\partial^2 w}{\partial\beta^2}\Big|_{\beta=0}\sin(\lambda_m\alpha)\mathrm{d}\alpha$$
$$K_{na}=\int_0^b\frac{\partial u}{\partial\alpha}\Big|_{\alpha=a}\sin(\gamma_n\beta)\mathrm{d}\beta,\quad K_{n0}=\int_0^b\frac{\partial u}{\partial\alpha}\Big|_{\alpha=0}\sin(\gamma_n\beta)\mathrm{d}\beta \tag{21}$$
$$L_{mb}=\int_0^a\frac{\partial v}{\partial\beta}\Big|_{\beta=b}\sin(\lambda_m\alpha)\mathrm{d}\alpha,\quad L_{m0}=\int_0^a\frac{\partial v}{\partial\beta}\Big|_{\beta=0}\sin(\lambda_m\alpha)\mathrm{d}\alpha$$

It follows from Eqs. (18)–(20) that

$$\left\{\begin{array}{c}\overline{u}_{\rm cs}\\ \overline{v}_{\rm sc}\\ \overline{w}_{\rm ss}\end{array}\right\}=\mathbf{T}\left\{\begin{array}{l}(-1)^m K_{na}-K_{n0}-\dfrac{1-\mu^2}{E\delta}\overline{q}_{\rm 1cs}\\ (-1)^n L_{mb}-L_{m0}-\dfrac{1-\mu^2}{E\delta}\overline{q}_{\rm 2sc}\\ \dfrac{\delta^2}{12}\{\lambda_m[(-1)^m I_{na}-I_{n0}]+\gamma_n[(-1)^n J_{mb}-J_{m0}]\}+\dfrac{1-\mu^2}{E\delta}\overline{q}_{\rm 3ss}\end{array}\right\} \tag{22}$$

where the symbolic matrix $\mathbf{T}$ is written as

$$\mathbf{T}=\left[\begin{array}{ccc}\lambda_m^2+\dfrac{1-\mu}{2}\gamma_n^2 & \frac{1+\mu}{2}\lambda_m\gamma_n & -\frac{\mu}{R}\lambda_m\\ \dfrac{1+\mu}{2}\lambda_m\gamma_n & \frac{1-\mu}{2}\lambda_m^2+\gamma_n^2 & -\frac{1}{R}\gamma_n\\ -\dfrac{\mu}{R}\lambda_m & -\frac{1}{R}\gamma_n & \frac{1}{R^2}+\frac{\delta^2}{12}\left(\lambda_m^2+\gamma_n^2\right)^2\end{array}\right]^{-1} \tag{23}$$

Equation (22) establishes the relationship between the transforms of the three displacements and eight sets of unknowns as defined by Eq. (21).

From Eq. (13), incorporating the Stokes transformation (Khalili et al., 2005) for differentiation of trigonometric series, we have

$$\frac{\partial w}{\partial\alpha}=\frac{2}{ab}\sum_{m=0}^{\infty}\sum_{n=1}^{\infty}\varepsilon_m\left\{\int_0^b[w\cos(\lambda_m\alpha)]\big|_0^a\sin(\gamma_n\beta)\mathrm{d}\beta+\lambda_m\overline{w}_{ss}\right\}\cos(\lambda_m\alpha)\sin(\gamma_n\beta)$$
$$\frac{\partial w}{\partial\beta}=\frac{2}{ab}\sum_{m=1}^{\infty}\sum_{n=0}^{\infty}\varepsilon_n\left\{\int_0^a[w\cos(\gamma_n\beta)]\big|_0^b\sin(\lambda_m\alpha)\mathrm{d}\alpha+\gamma_n\overline{w}_{ss}\right\}\sin(\lambda_m\alpha)\cos(\gamma_n\beta) \tag{24}$$

Noting $w|_{\alpha=0,a}=0$ and $w|_{\beta=0,b}=0$, substitution of Eqs. (13) and (24) into the remaining eight boundary conditions that have not been employed, i.e., $u|_{\alpha=0,a}=0$, $v|_{\beta=0,b}=0$, $\partial w/\partial\alpha|_{\alpha=0,a}=0$, and $\partial w/\partial\beta|_{\beta=0,b}=0$, we have

$$\frac{2}{ab}\sum_{m=0}^{\infty}\sum_{n=1}^{\infty}\varepsilon_m\overline{u}_{cs}\cos(\lambda_m\alpha)\sin(\gamma_n\beta)\Big|_{\alpha=0,a}=0$$
$$\frac{2}{ab}\sum_{m=1}^{\infty}\sum_{n=0}^{\infty}\varepsilon_n\overline{v}_{sc}\sin(\lambda_m\alpha)\cos(\gamma_n\beta)\Big|_{\beta=0,b}=0$$
$$\frac{4}{ab}\sum_{m=1}^{\infty}\sum_{n=1}^{\infty}\lambda_m\overline{w}_{ss}\cos(\lambda_m\alpha)\sin(\gamma_n\beta)\Big|_{\alpha=0,a}=0 \tag{25}$$
$$\frac{4}{ab}\sum_{m=1}^{\infty}\sum_{n=1}^{\infty}\gamma_n\overline{w}_{ss}\sin(\lambda_m\alpha)\cos(\gamma_n\beta)\Big|_{\beta=0,b}=0$$

Due to the orthogonality of trigonometric functions, we have

$$\begin{array}{ll}\sum_{m=0}^{\infty}\varepsilon_m\overline{u}_{\rm cs}=0 & \text{for } n=1,2,3,\cdots\\ \sum_{m=0}^{\infty}(-1)^m\varepsilon_m\overline{u}_{\rm cs}=0 & \text{for } n=1,2,3,\cdots\\ \sum_{n=0}^{\infty}\varepsilon_n\overline{v}_{\rm sc}=0 & \text{for } m=1,2,3,\cdots\\ \sum_{n=0}^{\infty}(-1)^n\varepsilon_n\overline{v}_{\rm sc}=0 & \text{for } m=1,2,3,\cdots\\ \sum_{m=1}^{\infty}\lambda_m\overline{w}_{\rm ss}=0 & \text{for } n=1,2,3,\cdots\\ \sum_{m=1}^{\infty}(-1)^m\lambda_m\overline{w}_{\rm ss}=0 & \text{for } n=1,2,3,\cdots\\ \sum_{n=1}^{\infty}\gamma_n\overline{w}_{\rm ss}=0 & \text{for } m=1,2,3,\cdots\\ \sum_{n=1}^{\infty}(-1)^n\gamma_n\overline{w}_{\rm ss}=0 & \text{for } m=1,2,3,\cdots\end{array} \tag{26}$$

Substituting Eq. (22) into Eq. (26), we obtain eight infinite systems of linear simultaneous equations with respect to the eight sets of unknowns as defined by Eq. (21). In actual computation, finite series terms should be taken. In other words, instead of ∞, the prescribed positive integers, M and N, can be taken in Eq. (26) as the upper limits of m and n, respectively. Accordingly, we have $4(M+N)$ equations with the same number of solvable constants, i.e., I_{n0}, I_{na}, K_{n0}, K_{na} ($n=1,2,3,\cdots,N$) and J_{m0}, J_{mb}, L_{m0}, L_{mb} ($m=1,2,3,\cdots,M$). Substituting the determined constants into Eq. (22) then into Eq. (13) leads to the analytical displacement solutions of CCCC cylindrical shell panels. Any other mechanical quantities can be further obtained. For instance, the internal forces can be readily pursued by Eqs. (4)–(11).

3. Cylindrical shell panels with other combinations of clamped and simply supported edges

To further demonstrate the generality of the present double finite integral transform method, we explore the analytical solutions of non-Lévy-type cylindrical shell panels with other combinations of clamped and simply supported edges.

For a CCCS panel, the edge at $\alpha=0$ is simply supported and the other three edges are clamped; thus, the boundary conditions are written as

$$\begin{array}{l}(F_{T1},v,w,M_1)|_{\alpha=0}=0\\ \left(u,v,w,\dfrac{\partial w}{\partial\alpha}\right)\Big|_{\alpha=a}=0\\ \left(u,v,w,\dfrac{\partial w}{\partial\beta}\right)\Big|_{\beta=0}=0\\ \left(u,v,w,\dfrac{\partial w}{\partial\beta}\right)\Big|_{\beta=b}=0\end{array} \tag{27}$$

Compared with the derivation of the CCCC panel, the new conditions

$$F_{T1}|_{\alpha=0} = \frac{E\delta}{1-\mu^2}\left[\frac{\partial u}{\partial \alpha}+\mu\left(\frac{\partial v}{\partial \beta}+\frac{w}{R}\right)\right]\Big|_{\alpha=0} = 0$$
$$M_1|_{\alpha=0} = -\frac{E\delta^3}{12(1-\mu^2)}\left(\frac{\partial^2 w}{\partial \alpha^2}+\mu\frac{\partial^2 w}{\partial \beta^2}\right)\Big|_{\alpha=0} = 0 \tag{28}$$

yield

$$I_{n0} = \int_0^b \frac{\partial^2 w}{\partial \alpha^2}\Big|_{\alpha=0} \sin(\gamma_n\beta)\mathrm{d}\beta = 0$$
$$K_{n0} = \int_0^b \frac{\partial u}{\partial \alpha}\Big|_{\alpha=0} \sin(\gamma_n\beta)\mathrm{d}\beta = \int_0^b \left(-\mu\frac{\partial v}{\partial \beta}\right)\Big|_{\alpha=0}$$
$$\sin(\gamma_n\beta)\mathrm{d}\beta = -\mu\left[sin(\gamma_n\beta)v|_{\alpha=0}\right]\Big|_0^b + \mu\gamma_n\int_0^b v|_{\alpha=0}\cos(\gamma_n\beta)\mathrm{d}\beta = 0 \tag{29}$$

Therefore, a simplification of Eq. (22) gives

$$\begin{Bmatrix}\overline{u}_{cs}\\ \overline{v}_{sc}\\ \overline{w}_{ss}\end{Bmatrix} = \mathbf{T}\begin{Bmatrix}(-1)^m K_{na} - \dfrac{1-\mu^2}{E\delta}\overline{q}_{1cs}\\ (-1)^n L_{mb} - L_{m0} - \dfrac{1-\mu^2}{E\delta}\overline{q}_{2sc}\\ \dfrac{\delta^2}{12}\{(-1)^m\lambda_m I_{na} + \gamma_n[(-1)^n J_{mb} - J_{m0}]\} + \dfrac{1-\mu^2}{E\delta}\overline{q}_{3ss}\end{Bmatrix} \tag{30}$$

Following the same logic as depicted in section 2.3, satisfying the remaining six boundary conditions yields six infinite systems of linear simultaneous equations with respect to the six sets of unknowns. Substituting the determined constants into Eq. (30) then into Eq. (13) leads to the analytical solutions of CCCS panels. The solutions for the other cases can be obtained with the same procedure. For the sake of brevity, only the boundary conditions and the relationships between the transforms of the three displacements and the unknowns are presented.

For a SCCC panel, the boundary conditions are

$$\left(u, v, w, \frac{\partial w}{\partial \alpha}\right)\Big|_{\alpha=0} = 0$$
$$\left(u, v, w, \frac{\partial w}{\partial \alpha}\right)\Big|_{\alpha=a} = 0$$
$$(F_{T2}, v, w, M_2)|_{\beta=0} = 0 \tag{31}$$
$$\left(u, v, w, \frac{\partial w}{\partial \beta}\right)\Big|_{\beta=b} = 0$$

The corresponding relationship is

$$\begin{Bmatrix}\overline{u}_{cs}\\ \overline{v}_{sc}\\ \overline{w}_{ss}\end{Bmatrix} = \mathbf{T}\begin{Bmatrix}(-1)^m K_{na} - K_{n0} - \dfrac{1-\mu^2}{E\delta}\overline{q}_{1cs}\\ (-1)^n L_{mb} - \dfrac{1-\mu^2}{E\delta}\overline{q}_{2sc}\\ \dfrac{\delta^2}{12}\{\lambda_m[(-1)^m I_{na} - I_{n0}] + (-1)^n\gamma_n J_{mb}\} + \dfrac{1-\mu^2}{E\delta}\overline{q}_{3ss}\end{Bmatrix} \tag{32}$$

For a SCCS panel, the boundary conditions are

$$(F_{T1}, v, w, M_1)|_{\alpha=0} = 0$$
$$\left(u, v, w, \frac{\partial w}{\partial \alpha}\right)\Big|_{\alpha=a} = 0$$
$$(F_{T2}, v, w, M_2)|_{\beta=0} = 0 \tag{33}$$
$$\left(u, v, w, \frac{\partial w}{\partial \beta}\right)\Big|_{\beta=b} = 0$$

The corresponding relationship is

$$\begin{Bmatrix}\overline{u}_{cs}\\ \overline{v}_{sc}\\ \overline{w}_{ss}\end{Bmatrix} = \mathbf{T}\begin{Bmatrix}(-1)^m K_{na} - \dfrac{1-\mu^2}{E\delta}\overline{q}_{1cs}\\ (-1)^n L_{mb} - \dfrac{1-\mu^2}{E\delta}\overline{q}_{2sc}\\ \dfrac{\delta^2}{12}[(-1)^m\lambda_m I_{na} + (-1)^n\gamma_n J_{mb}] + \dfrac{1-\mu^2}{E\delta}\overline{q}_{3ss}\end{Bmatrix} \tag{34}$$

4. Comprehensive numerical results with validations

Comprehensive numerical results of CCCC, SCCC, CCCS, and SCCS cylindrical shell panels with $R/a = 1$, $b/a = 1$ and uniform radial loading of intensity q are given to reveal the validity of this study. The non-dimensional displacement solutions, $\widehat{u} = 10^7 uE\delta^3/(qa^4)$, $\widehat{v} = 10^7 vE\delta^3/(qa^4)$, and $\widehat{w} = 10^7 wE\delta^3/(qa^4)$, and non-dimensional bending moments, $\widehat{M}_1 = 10^5 M_1/(qa^2)$ and $\widehat{M}_2 = 10^5 M_2/(qa^2)$, are adopted.

The convergence study of CCCC panels is first carried out for the displacements and bending moments at typical locations, as shown in Tables 1 and 2, respectively, where the bold figures are the convergent ones. Overall, with the increase of the number of series terms, the displacement solutions converge fast whereas the bending moments converge slower since they are obtained by the second derivatives of w. Eventually, 400 series terms have been taken throughout to achieve the accuracy of four significant digits for all the displacement solutions, and 2000 series terms achieve the accuracy of three significant digits for all the bending moment solutions in this study. The FEM-based numerical solutions have been obtained by the ABAQUS software (ABAQUS, 2013) for comparison, where the Poisson's ratio and thickness-to-span ratio are set to be 0.3 and 10^{-3}, respectively. The adopted element is C3D20R solid element. A fine enough mesh is set, with the mesh size being 1/200 of a, which outputs numerical solutions with high accuracy. The results by an up-to-date symplectic superposition method (SSM) have also been presented for comparison (Zheng et al., 2019). Satisfactory agreement is found between the present analytical solutions and those by FEM as well as SSM, confirming the accuracy of the analytical results.

Comprehensive non-dimensional displacement solutions of CCCC, CCCS, and SCCC panels are tabulated in Tables 3–5, respectively. $\widehat{u}$, $\widehat{v}$, and $\widehat{w}$ of SCCS panels are tabulated in Tables 6–8, respectively. The non-dimensional bending moments of CCCC, CCCS, and SCCC panels are tabulated in Tables 9–11, respectively. Tables 12 and 13 present $\widehat{M}_1$ and $\widehat{M}_2$ of SCCS panels. Overall, 408 displacements and 392 bending moments at different locations have been listed to provide comprehensive benchmark numerical results. All the present analytical solutions agree well with the reference ones. Compared with the analytical SSM that involves unusual mathematical skills (Zheng et al., 2019), the present finite integral transform method is more straightforward, which provides an easy-to-implement tool for analytical modeling of similar mechanics problems.

5. Concluding remarks

This study demonstrates the analytical double finite integral transform method for static bending problems of cylindrical shell panels. The theoretical foundation of the method is solid and the solution procedure is succinct without introducing any abstruse mathematical skills, which qualifies the method as a promising straightforward tool that may attract more extensive applications than some other analytical methods. In view of the merits on dealing with complex boundary-value problems of high-order PDEs, the follow-up studies on the method may be oriented towards more difficult issues such as bending, vibration, and buckling of intricate shell structures.

It is worth pointing out that the double finite integral transform method is also applicable to the panels with free edge(s), although this study focuses on those without a free edge. However, different integral transform kernels may be adopted. In general, taking the displacement w

as an example, one could follow the guidelines below to choose the kernels provided that a similar coordinate system to this study is taken. For a pair of opposite edges, a sinusoidal kernel is adopted in the corresponding direction when the both edges are clamped or simply supported, or one of them is clamped and another simply supported; a half-sinusoidal/cosinusoidal kernel is adopted when one of them is clamped or simply supported and another free; a cosinusoidal kernel is adopted when the both edges are free. The panels in this study fall into the first category, thus the sinusoidal kernels are adopted in both directions for w.

Declaration of competing interests

The authors declare that they have no known competing financial interests or personal relationships that could have appeared to influence the work reported in this paper.

Acknowledgements

The authors gratefully acknowledge the support from the National Natural Science Foundation of China (Grant Nos. 11972103 and 11825202) and Liaoning Revitalization Talents Program (Grant Nos. XLYC1807126 and XLYC1802020). Y.S. gratefully acknowledges the support from Beijing Municipal Science and Technology Commission (Z191100002019010), Beijing Municipal Natural Science Foundation (No. 2202066), Key Research Program of Frontier Sciences of the Chinese Academy of Sciences (ZDBS-LY-JSC014), Strategic Priority Research Program of the Chinese Academy of Sciences (No. XDB22040501), and State Key Laboratory of Structural Analysis for Industrial Equipment, Dalian University of Technology (No. GZ19102).

References

ABAQUS, 2013. Analysis User's Guide V6.13. Dassault Systèmes, Pawtucket, RI.
Achryya, A.K., Chakravorty, D., Karmakar, A., 2009. Bending characteristics of delaminated composite cylindrical shells - a finite element approach. J. Reinforc. Plast. Compos. 28, 965–978.
An, C., Su, J., 2011. Dynamic response of clamped axially moving beams: integral transform solution. Appl. Math. Comput. 218, 249–259.
Assaee, H., Hasani, H., 2015. Forced vibration analysis of composite cylindrical shells using spline finite strip method. Thin-Walled Struct. 97, 207–214.
Chen, S.W., Liu, H.M., Peng, Y., Sun, J.L., 2013. Strip layer method for simulation of the three-dimensional deformations of large cylindrical shell rolling. Int. J. Mech. Sci. 77, 113–120.
Cinefra, M., Belouettar, S., Soave, M., Carrera, E., 2010. Variable kinematic models applied to free-vibration analysis of functionally graded material shells. Eur. J. Mech. A Solid. 29, 1078–1087.
Cotta, R.M., Knupp, D.C., Naveira-Cotta, C.P., Sphaier, L.A., Quaresma, J.N.N., 2013. Unified integral transforms algorithm for solving multidimensional nonlinear convection-diffusion problems. Numer. Heat Tr.A-Appl. 63, 840–866.
Dirgantara, T., Aliabadi, M.H., 2012. Elastoplastic boundary element method for shear deformable shells. Eng. Struct. 45, 62–67.
Ferreira, A.J.M., Carrera, E., Cinefra, M., Roque, C.M.C., 2011. Analysis of laminated doubly-curved shells by a layerwise theory and radial basis functions collocation, accounting for through-the-thickness deformations. Comput. Mech. 48, 13–25.
He, Y., An, C., Su, J., 2020a. Generalized integral transform solution for free vibration of orthotropic rectangular plates with free edges. J. Brazilian Soc. Mech. Sci. Eng. 42, 183.
He, Y., An, C., Su, J., 2020b. Bending of orthotropic rectangular thin plates with two opposite edges clamped. Proc. Inst. Mech. Eng. Part C J. Mech. Eng. Sci. 234, 1220–1230.
Khalili, M.R., Malekzadeh, K., Mittal, R.K., 2005. A new approach to static and dynamic analysis of composite plates with different boundary conditions. Compos. Struct. 69, 149–155.
Leissa, A.W., 1973. Vibration of Shells. Scientific and Technical Information Office, National Aeronautics and Space Administration., Washington, D.C.
Li, H., Pang, F., Chen, H., 2019. A semi-analytical approach to analyze vibration characteristics of uniform and stepped annular-spherical shells with general boundary conditions. Eur. J. Mech. A Solid. 74, 48–65.
Li, R., Wang, H., Zheng, X., Xiong, S., Hu, Z., Yan, X., Xiao, Z., Xu, H., Li, P., 2019. New analytic buckling solutions of rectangular thin plates with two free adjacent edges by the symplectic superposition method. Eur. J. Mech. A Solid. 76, 247–262.
Li, R., Zhong, Y., Tian, B., Liu, Y., 2009. On the finite integral transform method for exact bending solutions of fully clamped orthotropic rectangular thin plates. Appl. Math. Lett. 22, 1821–1827.
Lim, C.W., Xu, X.S., 2010. Symplectic elasticity: theory and applications. Appl. Mech. Rev. 63, 050802.
Lim, C.W., Lü, C.F., Xiang, Y., Yao, W., 2009. On new symplectic elasticity approach for exact free vibration solutions of rectangular Kirchhoff plates. Int. J. Eng. Sci. 47, 131–140.
Matt, C.F.T., 2013. Combined classical and generalized integral transform approaches for the analysis of the dynamic behavior of a damaged structure. Appl. Math. Model. 37, 8431–8450.
Mousavi, S.M., Aghdam, M.M., 2009. Static bending analysis of laminated cylindrical panels with various boundary conditions using the differential cubature method. J. Mech. Mater. Struct. 4, 509–521.
Ortakaya, S., 2012. Exact solutions of the Klein - gordon equation with ring-shaped oscillator potential by using the Laplace integral transform. Chin. Phys. B 21, 070303.
Santos, E.N., Blanco, C.J.C., MacÊdo, E.N., Maneschy, C.E.A., Quaresma, J.N.N., 2012. Integral transform solutions for the analysis of hydrodynamic lubrication of journal bearings. Tribol. Int. 52, 161–169.
Silva, R.L., Quaresma, J.N.N., Santos, C.A.C., Cotta, R.M., 2011. Integral transforms solution for flow development in wavy wall ducts. Int. J. Numer. Method. H. 21, 219–243.
Sneddon, I.N., 1975. Application of Integral Transforms in the Theory of Elasticity. McGraw-Hill, New York.
Timoshenko, S., Woinowsky-Krieger, S., 1959. Theory of Plates and Shells. McGraw-Hill, Auckland.
Ullah, S., Wang, H., Zheng, X., Zhang, J., Zhong, Y., Li, R., 2019. New analytic buckling solutions of moderately thick clamped rectangular plates by a straightforward finite integral transform method. Arch. Appl. Mech. 89, 1885–1897.
Yang, X.J., 2016. A new integral transform method for solving steady heat-transfer problem. Therm. Sci. 20, S639–S642.
Zhang, J., Ullah, S., Zhong, Y., 2020. New analytical free vibration solutions of orthotropic rectangular thin plates using generalized integral transformation. J. Comput. Appl. Math. 367, 112439.
Zhang, S., Xu, L., Li, R., 2019. New exact series solutions for transverse vibration of rotationally-restrained orthotropic plates. Appl. Math. Model. 65, 348–360.
Zhang, X., Cai, J., Liu, L., Yang, Y., 2012. An integral transform and its applications in parameter estimation of LFM signals. Circ. Syst. Signal Process. 31, 1017–1031.
Zheng, X., Sun, Y., Huang, M., An, D., Li, P., Wang, B., Li, R., 2019. Symplectic superposition method-based new analytic bending solutions of cylindrical shell panels. Int. J. Mech. Sci. 152, 432–442.